

## Supporting Information

# Mechanism of Supplemental Activator and Reducing Agent Atom Transfer Radical Polymerization Mediated by Inorganic Sulfites: Experimental Measurements and Kinetic Simulations

Pawel Kryś,<sup>a</sup> Marco Fantin,<sup>a</sup> Patrícia V. Mendonça,<sup>b</sup> Carlos M. R. Abreu,<sup>a,b</sup> Tamaz Guliashvili,<sup>b</sup> Jaqueline Rosa,<sup>b</sup> Lino O. Santos,<sup>c</sup> Arménio C. Serra,<sup>b</sup> Krzysztof Matyjaszewski<sup>a\*</sup> and Jorge F. J. Coelho<sup>a,b\*</sup>

<sup>a</sup> Department of Chemistry, Carnegie Mellon University, 4400 Fifth Avenue, Pittsburgh, Pennsylvania 15213, United States

<sup>b</sup> CEMMPRE, Department of Chemical Engineering, University of Coimbra, 3030-790 Coimbra, Portugal

<sup>c</sup> CIEPQPF, Department of Chemical Engineering, Faculty of Sciences and Technology, University of Coimbra

**Typical polymerization procedure (SARA ATRP of MA (DP = 222) catalyzed by  $[\text{Na}_2\text{S}_2\text{O}_4]_0/[\text{Cu}^{\text{II}}\text{Br}_2]_0/[\text{Me}_6\text{TREN}]_0 = 1/0.1/0.1$  in MA/EtOH/ $\text{H}_2\text{O} = 2/0.9/0.1$  (v/v/v) mixture)**

Monomer (methyl acrylate, MA) was purified by passage through a sand/alumina column just before addition to the reaction. A mixture of  $\text{Cu}^{\text{II}}\text{Br}_2$  (6.7 mg, 0.030 mmol),  $\text{Me}_6\text{TREN}$  (6.9 mg, 0.03 mmol), EtOH (2.7 mL), and MilliQ  $\text{H}_2\text{O}$  (0.3 mL) (both previously bubbled with nitrogen for about 15 minutes) was placed in a Schlenk tube reactor sealed with a rubber septum. A mixture of MA (6.0 mL, 66.6 mmol) and EBiB (58.5 mg, 0.30 mmol) or MBrP (50.1 mg, 0.30 mmol) was added to the reactor and frozen in liquid nitrogen. The Schlenk tube reactor containing the reaction mixture was deoxygenated by five freeze-vacuum-thaw cycles and purged with nitrogen. Lastly,  $\text{Na}_2\text{S}_2\text{O}_4$  (52.3 mg, 0.30 mmol) was added to the reactor under nitrogen. The Schlenk tube reactor was placed in a water bath at 30 °C with stirring (600 rpm). Samples of the reaction mixture were collected periodically during the polymerization by using an airtight syringe and purging the side arm of the Schlenk tube reactor with nitrogen. The samples were analyzed by  $^1\text{H}$  NMR spectroscopy in order to determine the monomer conversion and by SEC to determine molecular weight and dispersity of the PMA.

**Determination of the reduction rate coefficient ( $k_{\text{red}}^{\text{app}}$ )**

A mixture of  $\text{Cu}^{\text{II}}\text{Br}_2$  (2.6 mg, 0.012 mmol),  $\text{Me}_6\text{TREN}$  (2.7 mg, 0.012 mmol), EtOH (1.05 mL), MilliQ  $\text{H}_2\text{O}$  (0.117 mL), and MeOAc (2.33 mL) (previously bubbled with nitrogen for about 15 minutes) was placed in a Quartz cuvette that was sealed with rubber septa. The initial UV-Vis spectrum was measured. Subsequently,  $\text{Na}_2\text{S}_2\text{O}_4$  (20.3 mg, 0.12 mmol) was added to the cuvette under nitrogen. The Quartz cuvette was placed in a water bath at 30 °C with stirring (600 rpm). The reaction mixture was centrifuged prior to the UV-Vis measurements in order to settle down the  $\text{Na}_2\text{S}_2\text{O}_4$  particles.

### Determination of rate coefficient of addition of $\text{SO}_2^{\bullet-}$ to the monomer ( $k_{i0}^{\text{app}}$ )

Monomer (methyl acrylate, MA) was purified by passage through a sand/alumina column just before addition to the reaction. A mixture of EtOH (2.7 mL), and MilliQ  $\text{H}_2\text{O}$  (0.3 mL) (both previously bubbled with nitrogen for about 15 minutes) was placed in a Schlenk tube reactor, sealed with a rubber septum. MA (6.0 mL, 66.6 mmol) was added to the reactor and frozen in liquid nitrogen. The Schlenk tube reactor containing the reaction mixture was deoxygenated with five freeze-vacuum-thaw cycles and purged with nitrogen. Lastly,  $\text{Na}_2\text{S}_2\text{O}_4$  (52.3 mg, 0.30 mmol) was added to the reactor under nitrogen. The Schlenk tube reactor was then placed in a water bath at 30 °C with stirring (600 rpm). Samples of the reaction mixture were collected periodically during the polymerization using an airtight syringe while purging the side arm of the Schlenk tube reactor with nitrogen. The samples were analyzed by  $^1\text{H}$  NMR spectroscopy to determine the monomer conversion and by SEC to determine molecular weight and dispersity of the PMA.

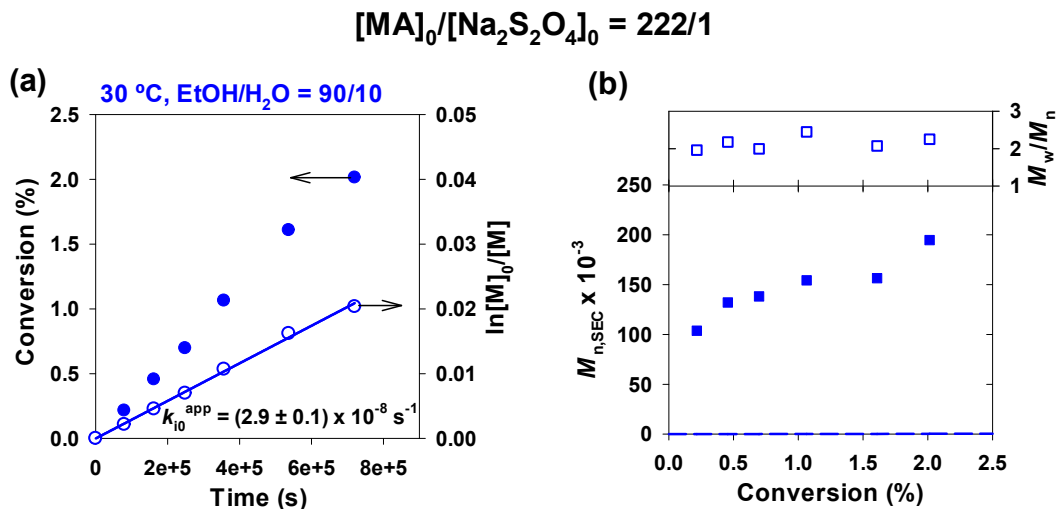


**Fig. S1.** (a) Monomer conversion and  $\ln[\text{M}]_0/[\text{M}]$  vs. time and (b) number-average molecular weight ( $M_n^{\text{SEC}}$ ) and dispersity ( $M_w/M_n$ ) vs. monomer conversion for the polymerization of MA in the presence of  $\text{Na}_2\text{S}_2\text{O}_4$  in EtOH/ $\text{H}_2\text{O}$  at 30°C. Conditions: MA/EtOH/ $\text{H}_2\text{O}$  = 2/0.9/0.1 (v/v/v);  $[\text{MA}]_0/[\text{Na}_2\text{S}_2\text{O}_4]_0 = 222/1$ ,  $[\text{MA}]_0 = 7.4 \text{ M}$ .

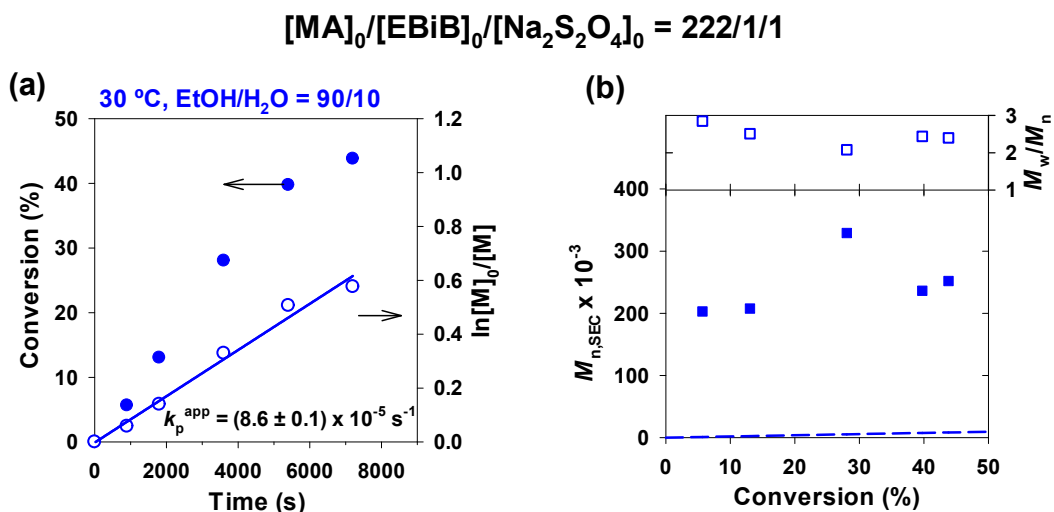


**Fig. S2.** (a) Monomer conversion and  $\ln[M]_0/[M]$  vs. time and (b) number-average molecular weight ( $M_n^{\text{SEC}}$ ) and dispersity ( $M_w/M_n$ ) vs. monomer conversion for the polymerization of MA in EtOH/H<sub>2</sub>O in the presence of Na<sub>2</sub>S<sub>2</sub>O<sub>4</sub> and EBiB at 30°C. Reaction conditions  $[\text{MA}]_0/[\text{EBiB}]_0/[\text{Na}_2\text{S}_2\text{O}_4]_0 = 222/1/1$ , MA/EtOH/H<sub>2</sub>O = 2/0.9/0.1 (v/v/v),  $[\text{MA}]_0 = 7.4$  M.

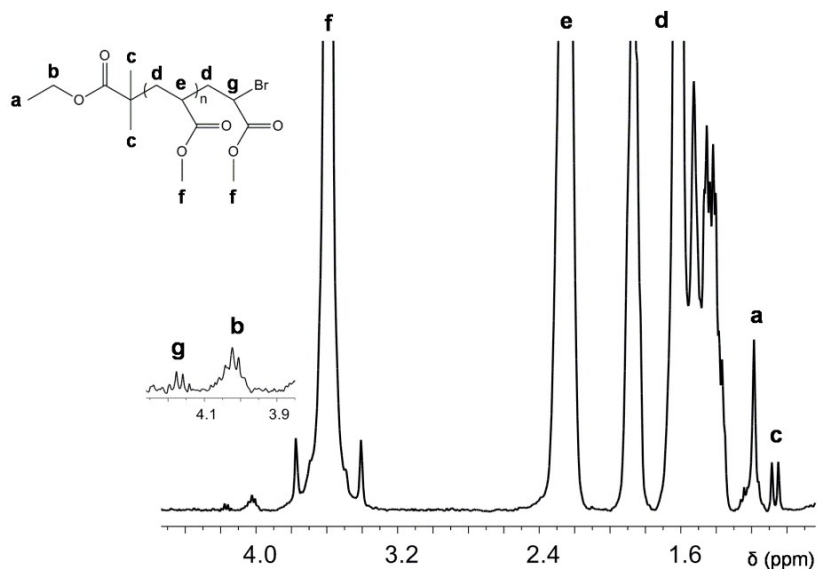


**Fig. S3.** <sup>1</sup>H NMR spectrum of a purified PMA sample ( $M_n^{\text{SEC}} = 3.2 \times 10^5$ ;  $\mathcal{D} = 5.2$ ). Reaction conditions:  $[\text{MA}]_0/[\text{EBiB}]_0/[\text{Na}_2\text{S}_2\text{O}_4]_0 = 20/1/1$  in EtOH/H<sub>2</sub>O = 0.9/0.1 (v/v) at 30°C;  $[\text{MA}]_0/[\text{solvent}] = 1/1$  (v/v).

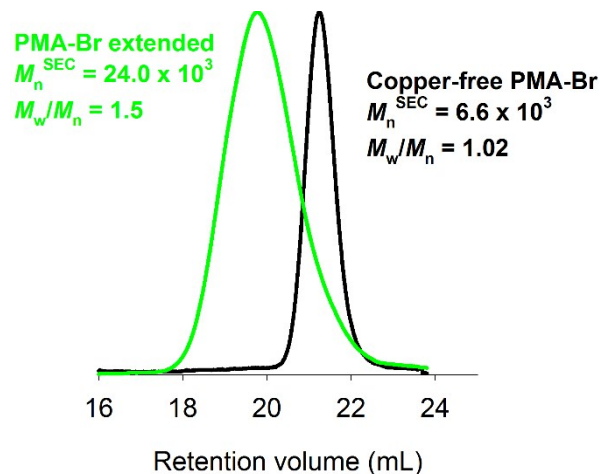


**Fig. S4.** SEC traces of a copper-free PMA-Br macroinitiator (black line) and chain extended polymer (green line) by SARA ATRP in EtOH/H<sub>2</sub>O = 0.9/0.1 (v/v) at 30°C. Conditions: [MA]<sub>0</sub>/[PMA-Br]<sub>0</sub>/[Na<sub>2</sub>S<sub>2</sub>O<sub>4</sub>]<sub>0</sub> = 200/1/1; [MA]<sub>0</sub>/[solvent] = 1/4 (v/v); time = 24 h; monomer conv. = 59%.

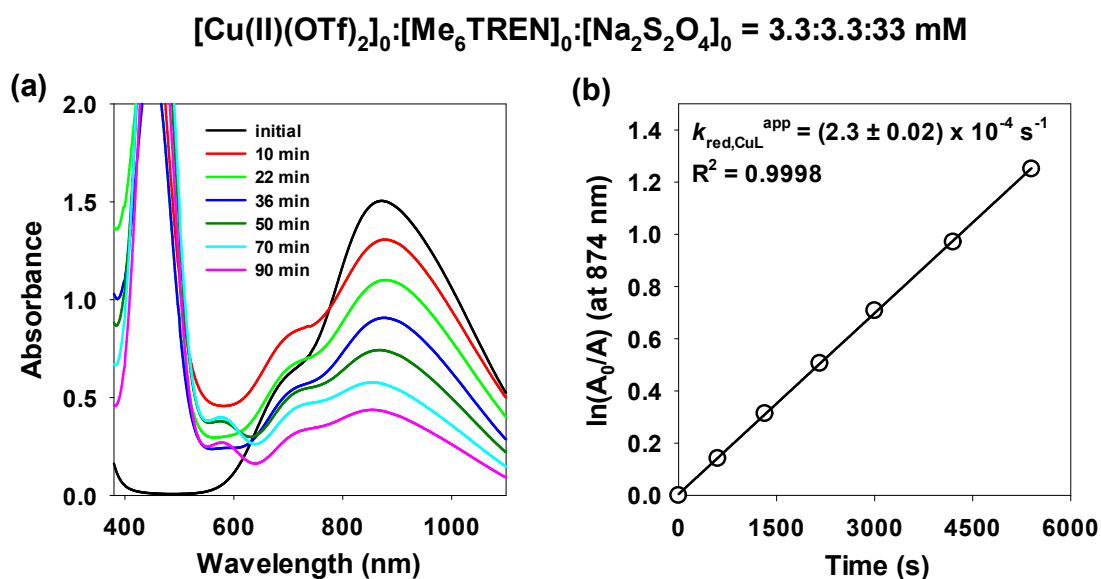


**Fig. S5.** (a) UV-Vis spectra of Cu<sup>II</sup>(OTf)<sub>2</sub>/Me<sub>6</sub>TREN during the reduction by Na<sub>2</sub>S<sub>2</sub>O<sub>4</sub> in a MeOAc/EtOH/H<sub>2</sub>O = 2/0.9/0.1 (v/v/v) mixture at 30 °C and (b) determination of the  $k_{\text{red,CuL}}^{\text{app}}$ . Conditions: [Cu<sup>II</sup>(OTf)<sub>2</sub>]<sub>0</sub>/[Me<sub>6</sub>TREN]<sub>0</sub>/[Na<sub>2</sub>S<sub>2</sub>O<sub>4</sub>]<sub>0</sub> = 0.1/0.1/1; [Cu<sup>II</sup>(OTf)<sub>2</sub>]<sub>0</sub> = 3.3 mM.

### Determination of $K_{\text{Br}^{\text{II}}}$

The equilibrium constant  $K_{\text{Br}^{\text{II}}}$  for association of bromide ions to  $\text{Cu}^{\text{II}}/\text{Me}_6\text{TREN}$  was determined by Vis-NIR spectrophotometric titration of the copper complex with  $\text{Et}_4\text{NBr}$  (Fig. S6). Spectra were recorded on an Agilent 8453 UV-Vis Spectrophotometer in a 1.00 cm quartz cuvette at *ca.* 25°C. The ionic strength was buffered by 0.1 M *n*- $\text{Bu}_4\text{NClO}_4$ . First, a  $2 \times 10^{-3}$  M  $\text{Cu}^{\text{II}}(\text{OTf})_2/\text{Me}_6\text{TREN}$  solution in  $\text{MA}/\text{EtOH}/\text{H}_2\text{O} = 2/0.9/0.1$  (v/v/v) was prepared in a cuvette ( $V_0 = 2.4$  mL), and a spectrum was recorded. Then, spectra were recorded after consecutive step-wise additions of a solution of  $\text{MA}/\text{EtOH}/\text{H}_2\text{O} = 2/0.9/0.1$  (v/v/v) containing  $2 \times 10^{-3}$  M  $\text{Cu}^{\text{II}}(\text{OTf})_2/\text{Me}_6\text{TREN}$  and  $2 \times 10^{-2}$  M *n*- $\text{Bu}_4\text{NBr}$ .

It was assumed that only two complexes were present in solution:  $\text{Cu}^{\text{II}}/\text{Me}_6\text{TREN}$  and  $\text{Cu}^{\text{II}}\text{Br}/\text{Me}_6\text{TREN}$ . The presence of a well-defined isosbestic point confirmed that only two copper species dominated the shape of the absorption spectra.

At the beginning of the experiment, mixing  $\text{Cu}^{\text{II}}(\text{OTf})_2$  and  $\text{Me}_6\text{TREN}$  generated only  $\text{Cu}^{\text{II}}/\text{Me}_6\text{TREN}$ , with a high formation constant,  $\log K = 27.2$  in acetonitrile<sup>1</sup> i.e.  $\text{Me}_6\text{TREN}$  is essentially quantitatively bonded to  $\text{Cu}^{2+}$ . On the other hand, the association of the weak  $\text{OTf}^-$  and  $\text{ClO}_4^-$  anions to copper was neglected. Solvent molecules that may be present in the  $\text{Cu}^{\text{II}}$  coordination sphere were also omitted.

Titration of  $\text{Cu}^{\text{II}}/\text{Me}_6\text{TREN}$  with *n*- $\text{Bu}_4\text{NBr}$ , from 0 to 7.5 mM, generated  $\text{Cu}^{\text{II}}\text{Br}/\text{Me}_6\text{TREN}$  as the main species. The formation of  $\text{Cu}^{\text{II}}/\text{Me}_6\text{TREN}$  complexes bearing more than one  $\text{Br}^-$  is unlikely because of the presence of a significant concentration of water, which significantly lowered the affinity of halide anions to copper.

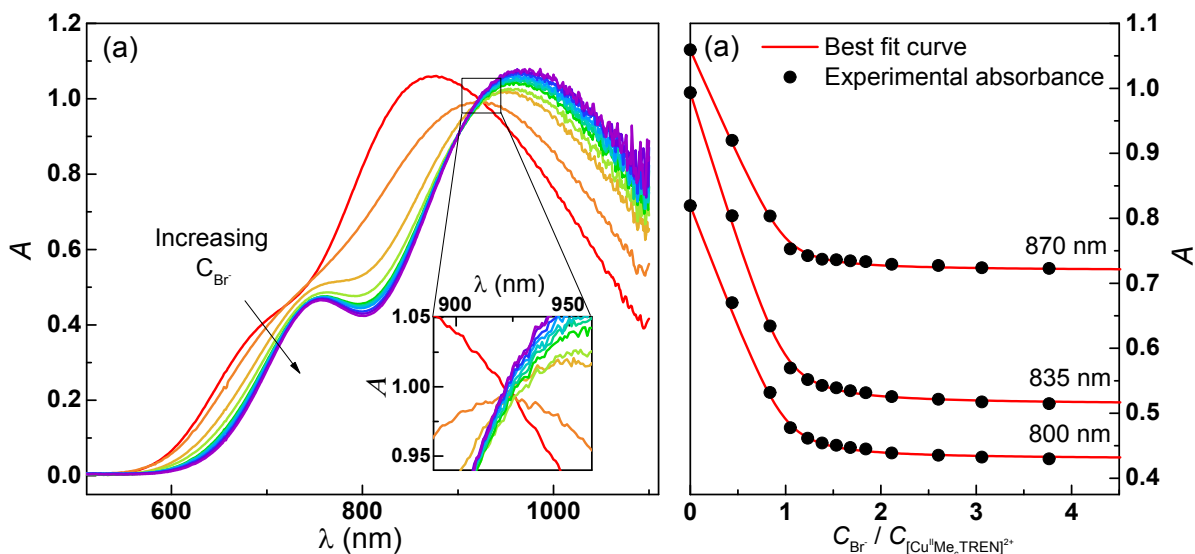


**Fig. S6.** a) Vis-NIR spectra of  $2 \times 10^{-3}$  M  $Cu^{II}(OTf)_2/Me_6TREN$  solutions at  $25^\circ C$  in  $MA/EtOH/H_2O = 2/0.9/0.1$  (v/v/v) +  $0.1$  M  $n-Bu_4NClO_4$ ,  $V_0 = 2.4$  mL; step additions (0 to 1.5 mL) of a solution containing  $2 \times 10^{-3}$  M  $Cu^{II}(OTf)_2/Me_6TREN$  and  $2 \times 10^{-2}$  M  $n-Bu_4NBr$  in  $MA/EtOH/H_2O = 2/0.9/0.1$  (v/v/v). (b) Absorbance values at three selected wavelengths and best-fit curves.

Recorded data were processed by MS Excel software. The Generalized Reduced Gradient (GRG) nonlinear algorithm was used to minimize the sum of the squared differences between experimental and calculated absorbance values. The program required the following inputs: the molar extinction coefficients of  $Cu^{II}/Me_6TREN$  at three different wavelengths ( $406 M^{-1} cm^{-1}$  @ 800 nm,  $493 M^{-1} cm^{-1}$  @ 835 nm, and  $525 M^{-1} cm^{-1}$  @ 870 nm), absorbance values in the absence and presence of various amount of  $n-Bu_4NBr$  (from 0 to 7.5 mM), and the concentration of all introduced species. The program outputs were: the  $Cu^{II}/Me_6TREN$  halidophilicity constant ( $K_{Br}^{II} = 1.65 \times 10^4 M^{-1}$ ), the molar extinction coefficient of  $Cu^{II}Br/Me_6TREN$  at each of the three selected wavelengths ( $215 M^{-1} cm^{-1}$  @ 800 nm,  $258 M^{-1} cm^{-1}$  @ 835 nm, and  $362 M^{-1} cm^{-1}$  @ 870 nm), a fitting of the calculated absorbance data with the experimental ones (Fig. S6b) and the squared sum of the differences between calculated and experimental absorbance values. From the last output, it was determined that the average difference between experimental and calculated values was very small ( $< 0.003$  absorbance units).

### Cyclic voltammetry (CV) of $\text{Cu}^{\text{II}}\text{Br}_2/\text{Me}_6\text{TREN}/\text{MBrP}$ at different scan rates

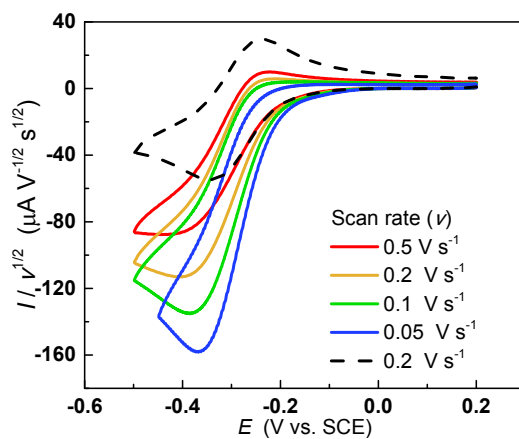


**Fig. S7.** CV of  $1.0 \times 10^{-3}$  M  $\text{Cu}^{\text{II}}\text{Br}_2/\text{Me}_6\text{TREN}$  in  $\text{MA}/\text{EtOH}/\text{H}_2\text{O} = 2/0.9/0.1$  (v/v/v) + 0.1 M  $n\text{-Bu}_4\text{NPF}_6$  at  $30^\circ\text{C}$  recorded at different scan rates in the absence (dashed line) and in the presence (solid lines) of  $2.0 \times 10^{-3}$  M MBrP ( $I$  was normalized by  $v^{1/2}$ ).

**Determination of  $k_{a1}$  for the reaction of  $\text{Cu}^{\text{I}}/\text{Me}_6\text{TREN}^+$  with MBrP and EBiB in  $\text{MeOAc}/\text{EtOH}/\text{H}_2\text{O} = 2/0.9/0.1$  (v/v/v)**

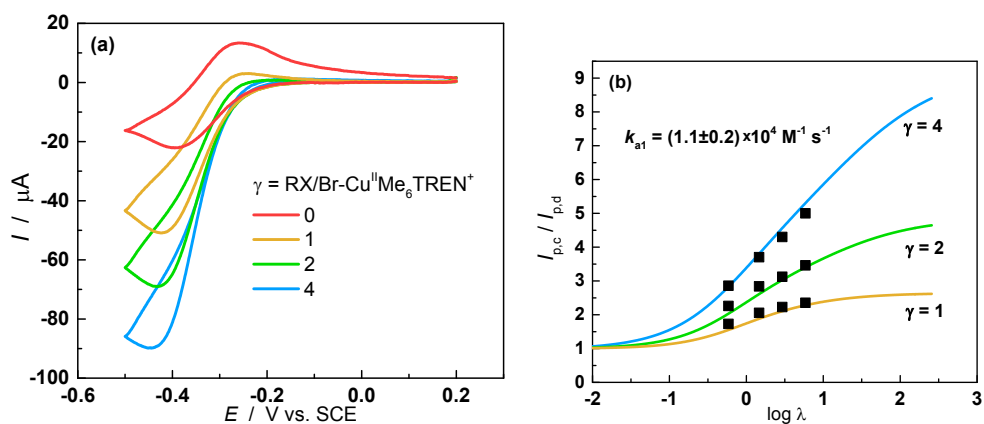


**Fig. S8.** (a) CV recorded at  $\nu = 0.2 \text{ V s}^{-1}$  for  $1.0 \text{ mM CuBr}_2/\text{Me}_6\text{TREN}$  in  $\text{MeOAc}/\text{EtOH}/\text{H}_2\text{O} = 2/0.9/0.1$  (v/v/v) in the absence and presence of MBrP  $30^\circ\text{C}$ . (b) Determination of  $k_{a1}$  for the reaction of  $\text{Cu}^{\text{I}}/\text{Me}_6\text{TREN}^+$  with MBrP in  $\text{MeOAc}/\text{EtOH}/\text{H}_2\text{O} = 2/0.9/0.1$  (v/v/v), by fitting of the experimental CV data on theoretical working curves at  $30^\circ\text{C}$ .

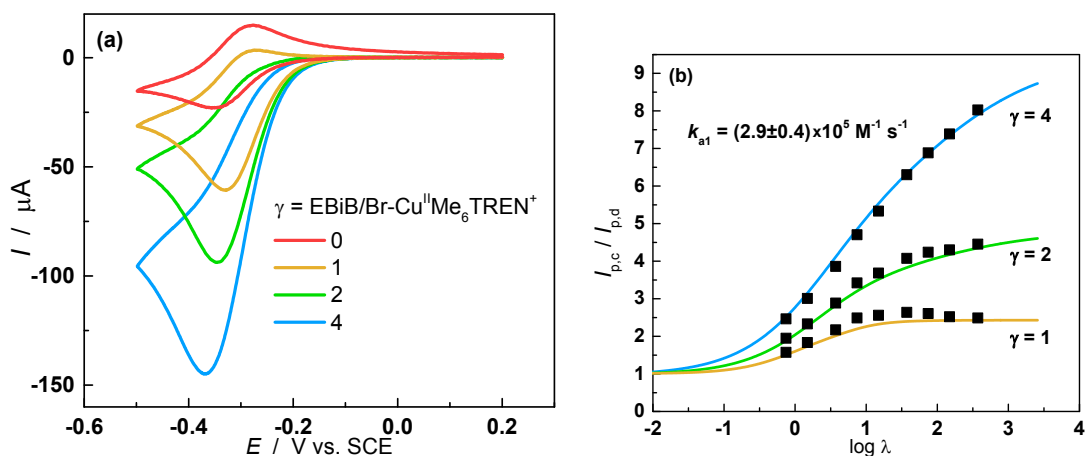


**Fig. S9.** (a) CV recorded at  $\nu = 0.2 \text{ V s}^{-1}$  for  $1.0 \text{ mM Cu}^{\text{II}}\text{Br}_2/\text{Me}_6\text{TREN}$  in  $\text{MeOAc}/\text{EtOH}/\text{H}_2\text{O} = 2/0.9/0.1$  (v/v/v) in the absence and presence of EBiB at  $30^\circ\text{C}$ . (b) Determination of  $k_{a1}$  for the reaction of  $\text{Cu}^{\text{I}}/\text{Me}_6\text{TREN}^+$  with EBiB in  $\text{MeOAc}/\text{EtOH}/\text{H}_2\text{O} = 2/0.9/0.1$  (v/v/v), by fitting of the experimental CV data on theoretical working curves at  $30^\circ\text{C}$ .

### Determination of $k_{a1}$ by comparison of $I_p/I_p^0$ data with theoretical working curves

Determination of  $k_{a1}$  was carried out using a similar procedure to that previously described in the literature.<sup>2</sup> The procedure first required creating theoretical  $I_p/I_p^0$  vs.  $\lambda$  curves, by simulating the CV of a catalytic mechanism as in Scheme 3. Then, the theoretical working curves were compared to the experimental  $I_p/I_p^0$  data.

### Determination of all parameters required for the simulation of CV

The CV of Cu<sup>II</sup>Br/Me<sub>6</sub>TREN was simulated with the software Digisim 3.03. The following reactions occur in the presence of an initiator and the radical scavenger 2,2,6,6-tetramethyl-1-piperidinyloxy (TEMPO). The relevant thermodynamic and kinetic parameters required for the simulation are listed in the same line:



The coupling reactions (Eq. S4) were considered to be very fast for all radicals, with rate constants  $k_{\text{T}} = 2.7 \times 10^8 \text{ M}^{-1} \text{ s}^{-1}$ .<sup>3-5</sup> The values for  $K_{\text{Br}}^{\text{I}}$  and  $K_{\text{ATRP}}$  were determined in this work and are listed in Table 1. Additionally, we assumed that the X<sup>-</sup> association/dissociation equilibria with Cu<sup>I</sup>/L are fast so that they constitute conditions of pre-equilibrium for the activation step ( $k_{\text{diss1}} = 3.07 \times 10^7 \text{ s}^{-1}$ , see Table 1). A value of  $k_{\text{diss1}}$  as low as of  $10^4 \text{ s}^{-1}$  did not alter the simulated voltammetric response. Note that reduction of the Cu<sup>II</sup>/L<sup>2+</sup> binary complex does not significantly contribute to the overall mechanism, because the complex is almost quantitatively bonded to Br<sup>-</sup>.

The standard reduction potential ( $E^{\circ}$ ) and the heterogeneous electron transfer rate constant ( $k^{\circ}$ ) of the complexes Cu<sup>II</sup>Br/L<sup>+</sup>, as well as the diffusion coefficients ( $D$ ) of all species,

were determined by CV. The Nichols method was applied to determine  $k^0$ .<sup>6</sup> Diffusion coefficients of the complexes were obtained from the cathodic peak current,  $I_{pc}$ , according to the following equation valid for a reversible electrode process:<sup>6</sup>

$$I_{pc} = (2.69 \times 10^5) n^{3/2} A D^{1/2} C \nu^{1/2} \quad (\text{Eq. S5})$$

where  $n$  is the number of exchanged electrons,  $A$  is the area of the electrode,  $\nu$  is the scan rate, and  $C$  is the bulk concentration of the  $\text{Cu}^{\text{II}}$  complex.

The initiators EBiB and MBrP gave a single irreversible reduction peak in CV corresponding to a  $2e^-$  reduction of the carbon-bromine bond to RH and  $\text{Br}^-$ . The peak current can be used also in this case to calculate  $D$  from the following equation:

$$I_{pc} = (2.99 \times 10^5) \alpha^{1/2} n A D^{1/2} C \nu^{1/2} \quad (\text{Eq. S6})$$

where  $C$  is the bulk concentration of RX and  $\alpha$  is the transfer coefficient, which was also determined from the peak characteristics according to known procedures.<sup>7</sup> The equation  $(\partial E_p)/\partial \log \nu = -1.15 RT/\alpha F$  was used, which relates the shift in the reduction peak potential,  $E_p$ , with  $\log \nu$ , to the transfer coefficient,  $\alpha$ . Values for  $\alpha = 0.29$  and  $0.31$  were determined for the reduction of MBrP and EBiB respectively, in  $\text{MeOAc}/\text{EtOH}/\text{H}_2\text{O} = 2/0.9/0.1$  (v/v/v). Table S1 summarizes all thermodynamic and kinetic data determined from CV for Cu complexes and initiators.

**Table S1.** Data from CV of  $[\text{Cu}^{\text{II}}\text{L}]^{2+}$  and RX in various reaction mixtures<sup>a</sup>

Species	MA/EtOH/H <sub>2</sub> O = 2/0.9/0.1 (v/v/v)			MA/EtOH/H <sub>2</sub> O = 2/1/0 (v/v/v)			MeOAc/EtOH/H <sub>2</sub> O = 2/0.9/0.1 (v/v/v)		
	$E^{\circ b}$	$10^6 D$	$10^3 k^{\circ}$	$E^{\circ b}$	$10^6 D$	$10^3 k^{\circ}$	$E^{\circ b}$	$10^6 D$	$10^3 k^{\circ}$
	(V)	(cm <sup>2</sup> /s)	(cm/s)	(V)	(cm <sup>2</sup> /s)	(cm/s)	(V)	(cm <sup>2</sup> /s)	(cm/s)
$\text{Cu}^{\text{II}}\text{Br}/\text{Me}_6\text{TREN}^+$	-0.289	5.9	0.01	-0.295	7.1	0.01	-0.315	7.2	0.02
EBiB	N/A <sup>c</sup>	15.6 <sup>d</sup>	N/A	-1.22 <sup>e</sup>	15.6 <sup>d</sup>	N/A	-1.22 <sup>f</sup>	15.6 <sup>d</sup>	N/A
MBrP	N/A <sup>c</sup>	17.8 <sup>d</sup>	N/A	-1.34 <sup>e</sup>	17.8 <sup>d</sup>	N/A	-1.34 <sup>f</sup>	17.8 <sup>d</sup>	N/A

<sup>a</sup> Data obtained at 30°C, using 0.1 M Bu<sub>4</sub>NPF<sub>6</sub> as supporting electrolyte. <sup>b</sup> vs saturated calomel electrode (SCE). <sup>c</sup> Not available because the onset of MA reduction was more positive than RX reduction. <sup>d</sup> The diffusion coefficient determined in MeOAc/EtOH/H<sub>2</sub>O = 2/0.9/0.1 (v/v/v) was used. <sup>e</sup> Measured in the presence of MeOAc because of the reduced electrochemical potential window in the presence of MA, due to reduction of the monomer. <sup>f</sup> Cathodic peak potential at  $\nu = 0.2 \text{ V s}^{-1}$ .

### Construction of the theoretical curves for homogenous redox catalysis and comparison with experimental $I_p/I_p^0$ data

$I_p/I_p^0$  depends on the following kinetic parameter

$$\lambda = \frac{RTk_{al}C_{[Cu^{II}L]^{2+}}}{F\nu}$$

where  $R$  is the gas constant,  $F$  is the Faraday constant,  $C_{[Cu^{II}L]^{2+}}$  is the bulk catalyst concentration and  $\nu$  is the scan rate. Theoretical curves relating  $I_p/I_p^0$  to  $\lambda$  can be constructed by digital simulation of the voltammetric response of the catalytic system, in agreement with the reaction mechanism in Eqs. S1-S4. Voltammetric simulations were carried out for a large number of  $\lambda$  values and the results were plotted as  $I_p/I_p^0$  versus  $\log \lambda$ . To accurately compare experimental and simulated data, the latter were first fit to an appropriate mathematical function that perfectly interpolated all simulated data (Eq. S7).

$$y = a + b \left[ \frac{c}{1 + \exp\left(\frac{x-d}{e}\right)} + \frac{1-c}{1 + \exp\left(\frac{x-f}{g}\right)} \right] \quad (\text{Eq. S7})$$

where  $a, b, c, d, e, f, g$  are fitting parameters.

The procedure used for determination of  $k_{al}$  follows. The CV experiment was carried out with fixed values of  $\gamma$ . Then a set of  $I_p/I_p^0$  versus  $\log \lambda' = RTk_{al}C_{[Cu^{II}L]^{2+}} / F\nu$  values were calculated for each  $\gamma$  value. The theoretical working curves were then constructed and fitted to Eq. S7 to define the constants in the equation. The experimental data were finally fitted to the



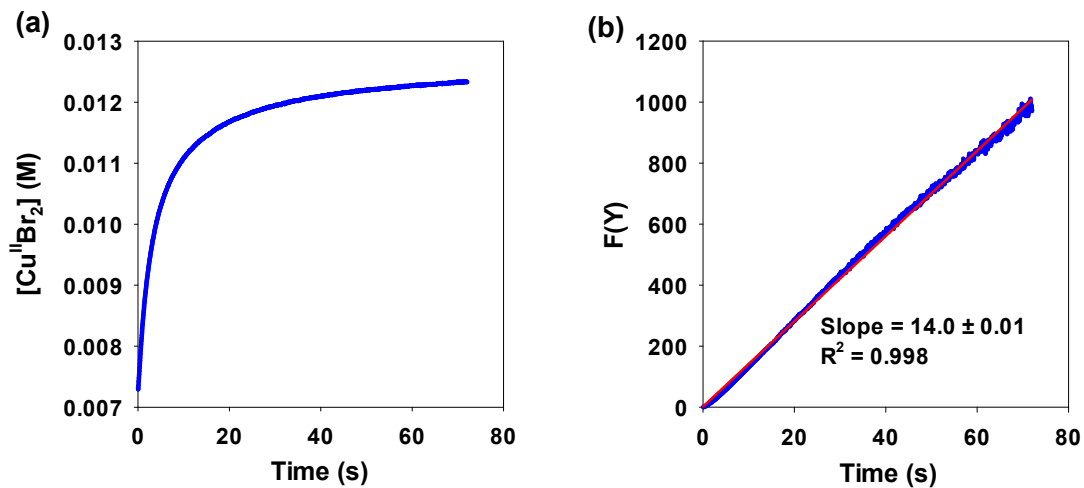


**Fig. S10.** Determination of  $K_{ATRP}$  value of CuBr/Me<sub>6</sub>TREN in MA/EtOH/H<sub>2</sub>O = 2/0.9/0.1 (v/v/v) with MBrP as the initiator. (a) Evolution of Cu<sup>II</sup>Br<sub>2</sub>/Me<sub>6</sub>TREN species; and (b) F(Y) function vs. time at 30°C.

$$slope = 14.0, K_{ATRP} = \sqrt{\frac{14.0}{2k_t}} = (1.7 \pm 0.05) \times 10^{-4}$$

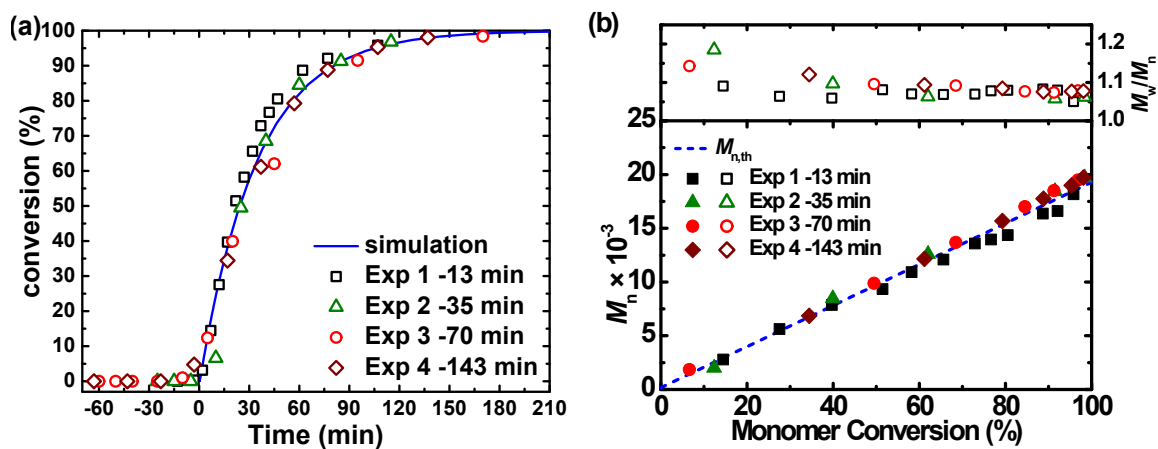


**Fig. S11.** (a) experimental (symbols) and simulated (lines) monomer conversion vs. time (with subtracted induction period), and (b) evolution of  $M_n$  and  $M_w/M_n$  with monomer conversion for SARA ATRP of MA under conditions  $[MA]_0/[MBrP]_0/[Na_2S_2O_4]_0/[Cu^{II}Br_2]_0/[Me_6TREN]_0 = 222/1/1/0.1/0.2$ ,  $[MA]_0 = 7.4$  M. MA/EtOH/H<sub>2</sub>O = 2/0.9/0.1 (v/v/v) at 30°C.

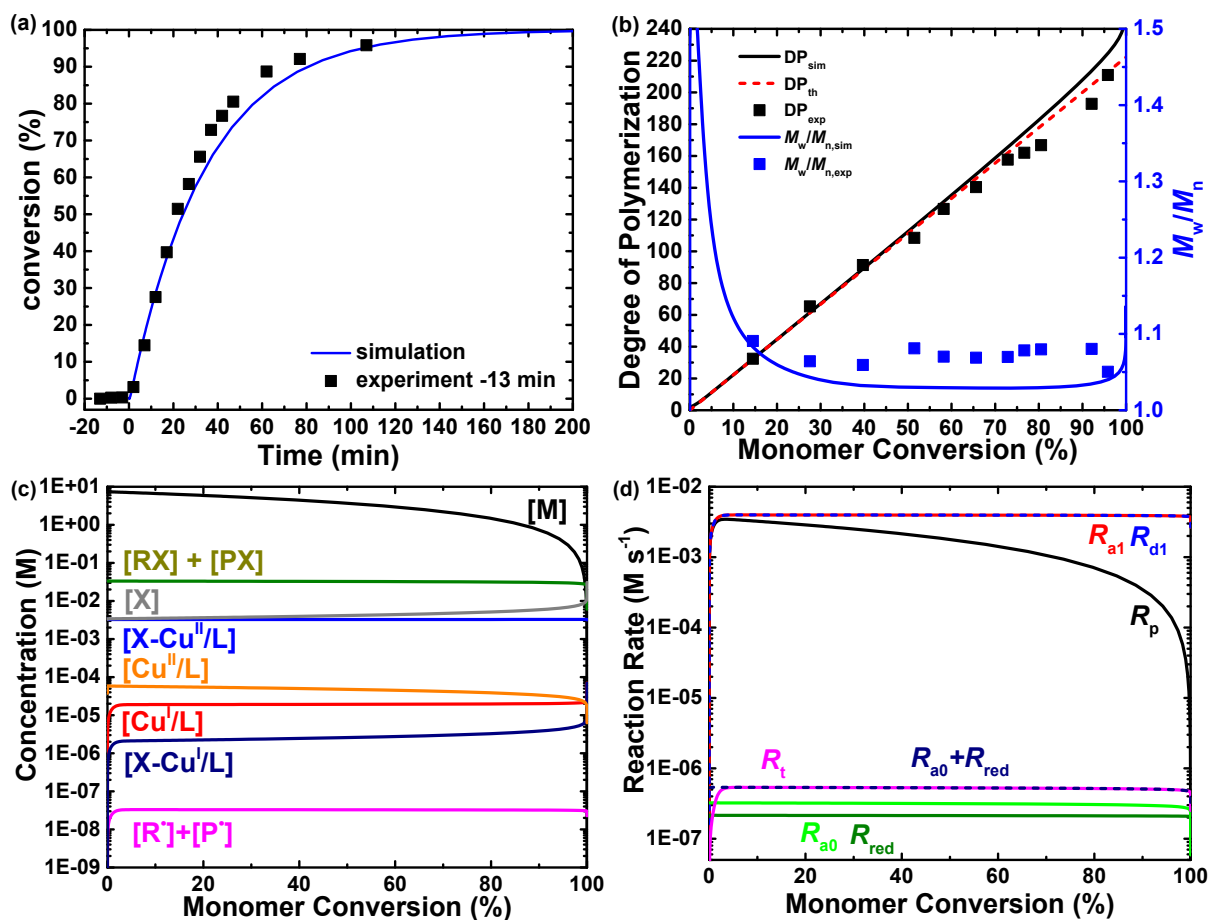


**Fig. S12.** Comparison of experimental data (symbols) with simulated results (lines) for SARA ATRP of MA in EtOH/H<sub>2</sub>O at 30°C. (a) monomer conversion vs. time, (b) number-average degree of polymerization ( $DP_n$ ) and  $\mathcal{D}$  ( $M_w/M_n$ ) vs. monomer conversion, (c) simulated concentration of species, and (d) calculated reaction rates. Reaction conditions: MA/EtOH/H<sub>2</sub>O = 2/0.9/0.1 (v/v/v);  $[MA]_0/[MBrP]_0/[Na_2S_2O_4]_0/[Cu^{II}Br_2]_0/[Me_6TREN]_0 = 222/1/1/0.1/0.2$ ,  $[MA]_0 = 7.4$  M.

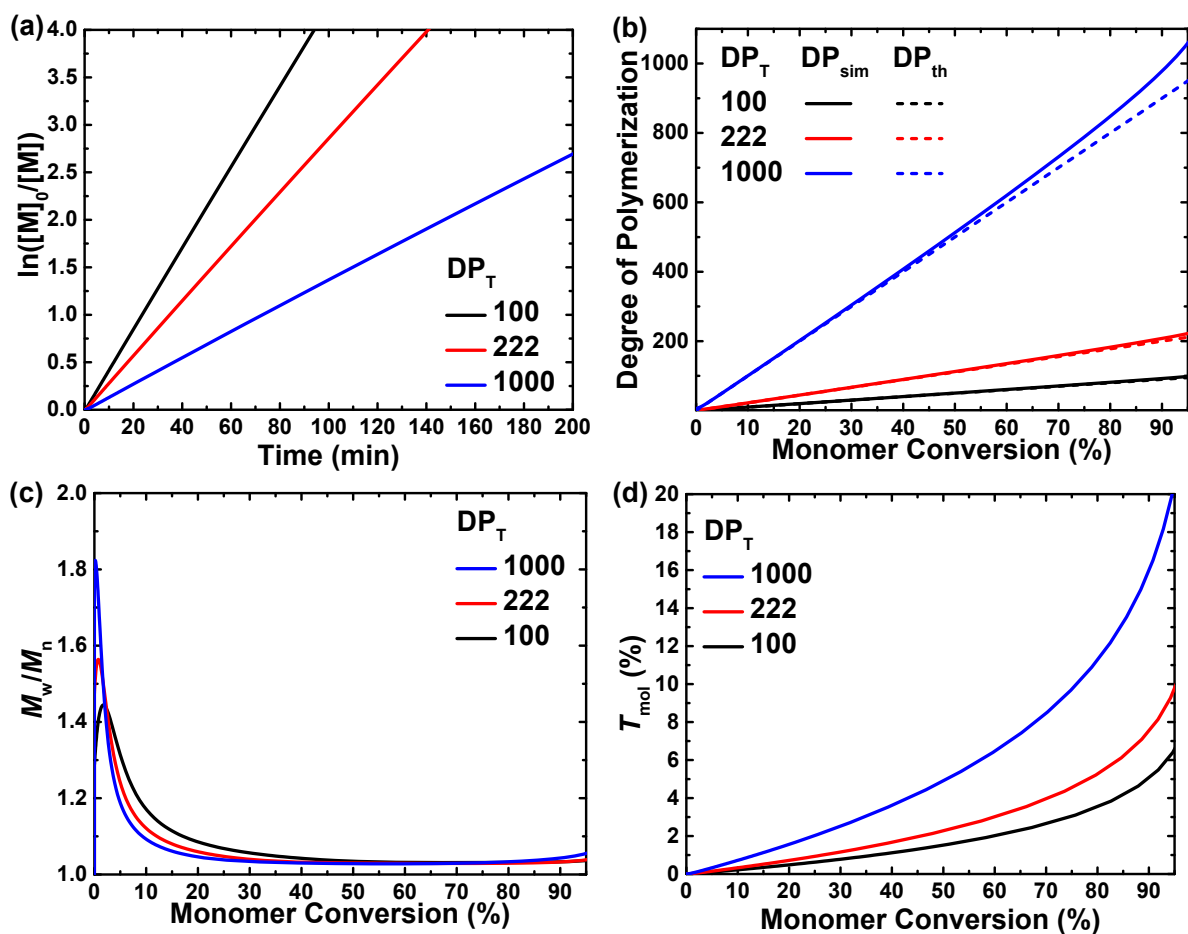


**Fig. S13.** Simulated kinetic plots for the SARA ATRP of MA in EtOH/H<sub>2</sub>O at 30°C. (a) semilogarithmic kinetic plot, (b) DP<sub>n</sub> vs. monomer conversion, (c)  $M_w/M_n$  vs. monomer conversion, and (d)  $T_{mol}$  vs. monomer conversion. Reaction conditions: MA/EtOH/H<sub>2</sub>O = 2/0.9/0.1 (v/v/v); [MA]<sub>0</sub>/[MBrP]<sub>0</sub>/[Na<sub>2</sub>S<sub>2</sub>O<sub>4</sub>]<sub>0</sub>/[Cu<sup>II</sup>Br<sub>2</sub>]<sub>0</sub>/[Me<sub>6</sub>TREN]<sub>0</sub> = DP<sub>n</sub>/1/1/0.1/0.2, where DP<sub>n</sub> = 100, 222, or 1000, [MA]<sub>0</sub> = 7.4 M.

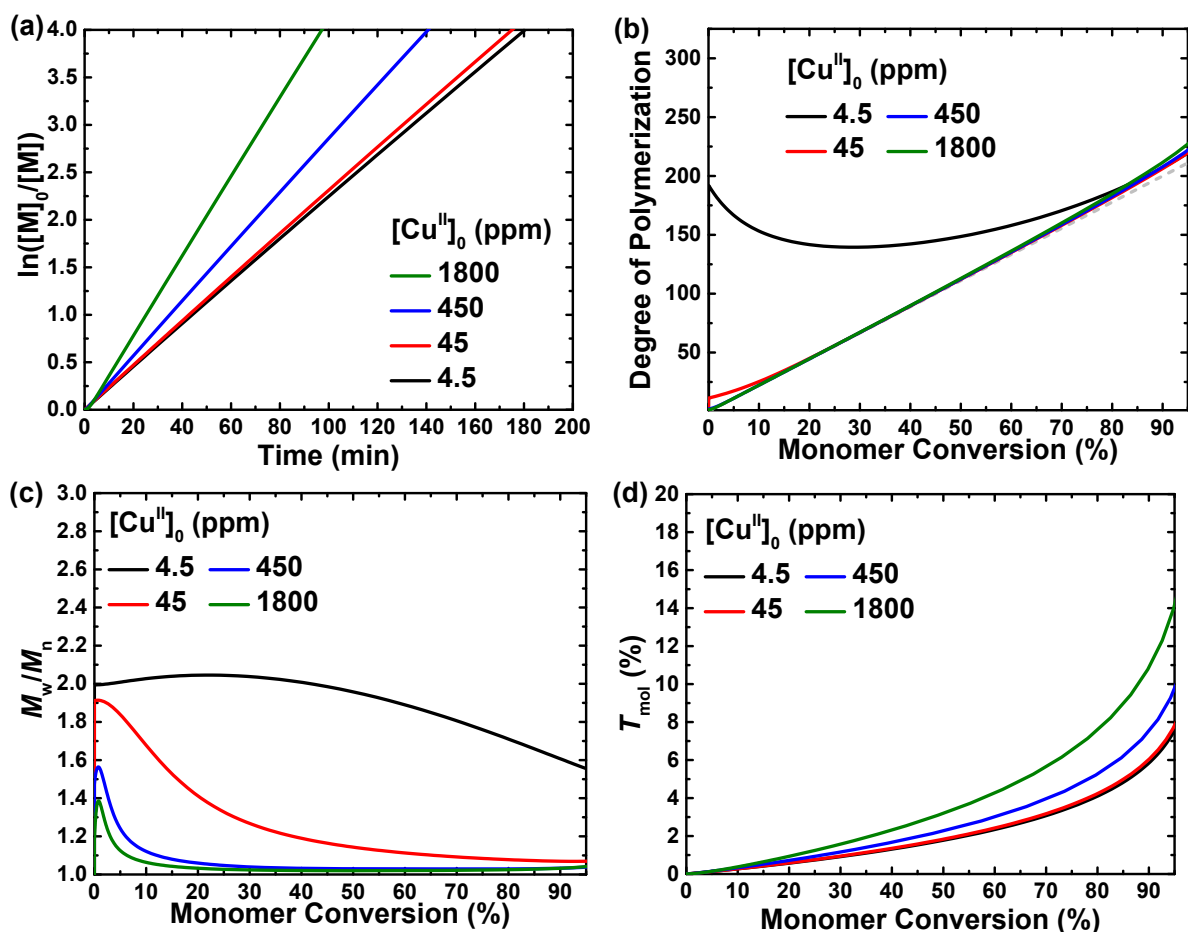


**Fig. S14.** Simulated kinetic plots for the SARA ATRP of MA in EtOH/H<sub>2</sub>O at 30°C. (a) semilogarithmic kinetic plot, (b)  $DP_n$  vs. monomer conversion, (c)  $M_w/M_n$  vs. monomer conversion, and (d)  $T_{mol\%}$  vs. monomer conversion. Reaction conditions: MA/EtOH/H<sub>2</sub>O = 2/0.9/0.1 (v/v/v); [MA]<sub>0</sub>/[MBrP]<sub>0</sub>/[Na<sub>2</sub>S<sub>2</sub>O<sub>4</sub>]<sub>0</sub>/[Cu<sup>II</sup>Br<sub>2</sub>]<sub>0</sub>/[Me<sub>6</sub>TREN]<sub>0</sub> = 222/1/1/x/2x, where x = 0.001, 0.01, 0.1 or 0.4, [MA]<sub>0</sub> = 7.4 M.

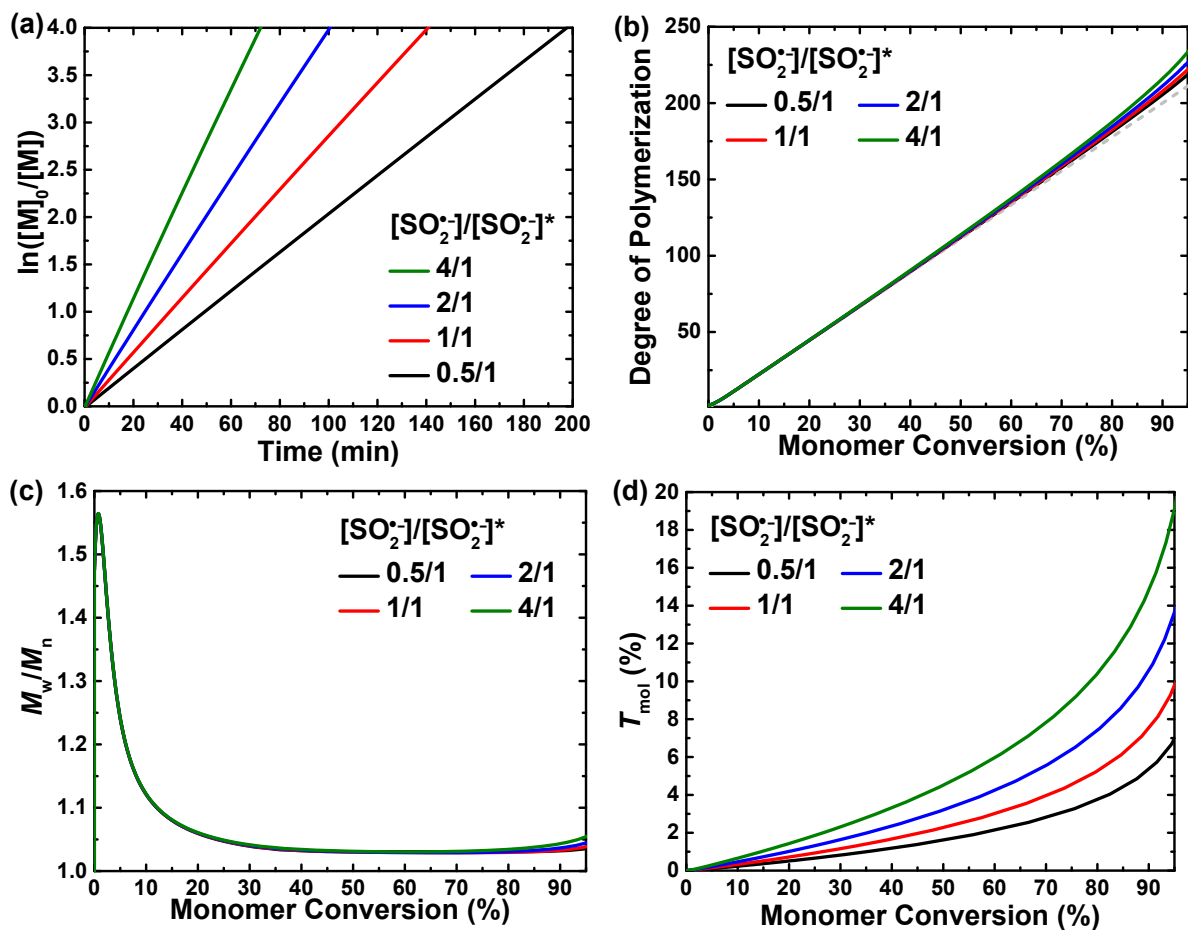


**Fig. S15.** Simulated kinetic plots for the SARA ATRP of MA in EtOH/H<sub>2</sub>O at 30°C. (a) semilogarithmic kinetic plot, (b) DP<sub>n</sub> vs. monomer conversion, (c)  $M_w/M_n$  vs. monomer conversion, and (d)  $T_{mol}$  vs. monomer conversion. Reaction conditions: MA/EtOH/H<sub>2</sub>O = 2/0.9/0.1 (v/v/v); [MA]<sub>0</sub>/[MBrP]<sub>0</sub>/[Cu<sup>II</sup>Br<sub>2</sub>]<sub>0</sub>/[Me<sub>6</sub>TREN]<sub>0</sub> = 222/1/0.1/0.2, with [SO<sub>2</sub><sup>•-</sup>]/[SO<sub>2</sub><sup>•-</sup>]\* = 0.5/1, 1/1, 2/1, and 4/1; [MA]<sub>0</sub> = 7.4 M.

### Scheme S1. Fundamental reactions constituting the ATRP equilibrium



The ATRP equilibrium (Eq. S11) can be expressed as the combination of three reactions (Eq. S8-S10), *i.e.* the dissociative electron transfer to RX (with reduction potential  $E_{\text{RX/R}^\bullet + \text{X}^-}^\circ$ ), the reversible electron transfer to the Cu complex ( $E_{[\text{Cu}^{\text{II}}\text{L}]^{2+} / [\text{Cu}^{\text{I}}\text{L}]^+}^\circ$ ) and the association of the halide anion to the Cu<sup>II</sup> complex with equilibrium constant  $K_{\text{X}}^{\text{II}}$ , (also termed halidophilicity constant). The effect of water on  $E_{[\text{Cu}^{\text{II}}\text{L}]^{2+} / [\text{Cu}^{\text{I}}\text{L}]^+}^\circ$  and on  $K_{\text{X}}^{\text{II}}$  was investigated as described in the main text.

### CV of Cu<sup>II</sup>/Me<sub>6</sub>TREN in MA and MA/EtOH = 2/1 (v/v)

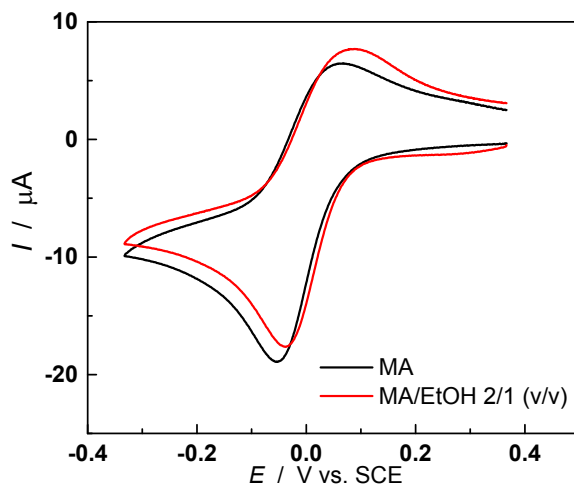


**Fig. S16.** CV of  $10^{-3}$  M  $\text{Cu}^{\text{II}}(\text{OTf})_2/\text{Me}_6\text{TREN}$  in MA and MA/EtOH = 2/1 (v/v) + 0.1 M *n*-Bu<sub>4</sub>NPF<sub>6</sub>.  $T = 30$  °C and  $\nu = 0.1$  V s<sup>-1</sup>.

### CV of Cu<sup>II</sup>Br/Me<sub>6</sub>TREN in different MA/EtOH/H<sub>2</sub>O mixtures

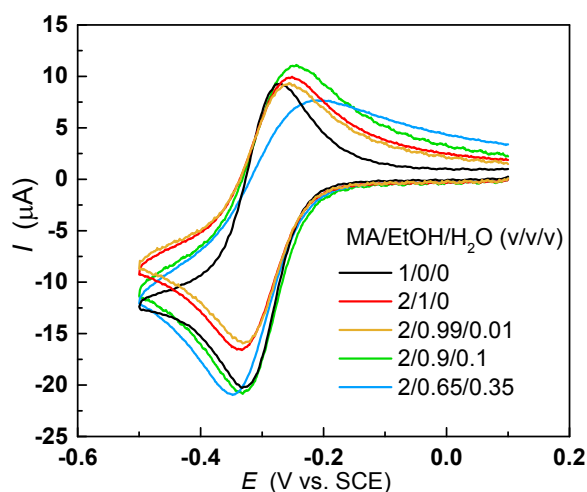


**Fig. S17.** CV of  $10^{-3}$  M Cu<sup>II</sup>Br<sub>2</sub>/Me<sub>6</sub>TREN in MA/EtOH/H<sub>2</sub>O at different volumetric ratios. The supporting electrolyte was 0.1 M *n*-Bu<sub>4</sub>NPF<sub>6</sub>.  $T = 30$  °C and  $\nu = 0.1$  V s<sup>-1</sup>.

### CV of Cu<sup>II</sup>Br/Me<sub>6</sub>TREN in water

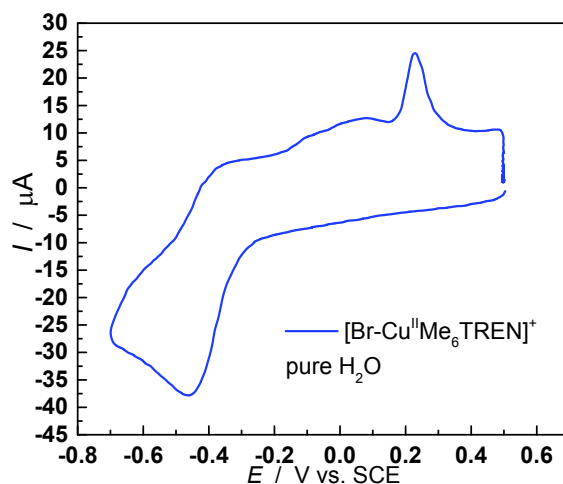


**Fig. S18.** CV of  $10^{-3}$  M Cu<sup>II</sup>(OTf)<sub>2</sub>/Me<sub>6</sub>TREN in water + 0.1 M Et<sub>4</sub>NBr. pH was adjusted to 6.8 with a buffer composed of tetraethyl ethylenediamine and HClO<sub>4</sub>. The Cu(I) complex was very unstable, which precluded accurate determination of its half-wave potential ( $E_{1/2}$ ). Note the excess of Br<sup>-</sup> added to have a sufficient amount of ternary complex Cu<sup>II</sup>Br/Me<sub>6</sub>TREN in pure water, due to the very low  $K_{Br}^{II}$ .

Determination of  $k_{a1}$  for the reaction of  $\text{Cu}^{\text{I}}/\text{Me}_6\text{TREN}^+$  with  $\text{MBrP}$  in  $\text{MA}/\text{EtOH} = 2/1$  (v/v)

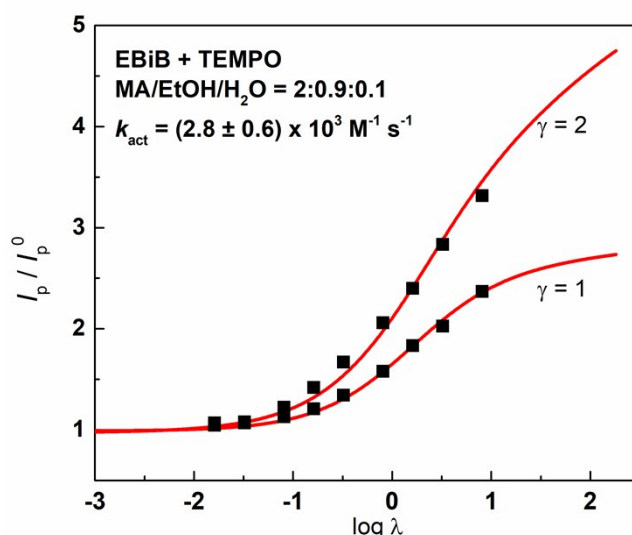


**Fig. S19.** Determination of  $k_{a1}$  for the reaction of  $\text{Cu}^{\text{I}}/\text{Me}_6\text{TREN}^+$  with  $\text{MBrP}$  in  $\text{MA}/\text{EtOH} = 2/1$  (v/v), by fitting of the experimental CV data on theoretical working curves at  $30^\circ\text{C}$ .

Determination of the reduction rate coefficient ( $k_{\text{red},\text{X-CuL}}^{\text{app}}$ ) for  $[\text{Cu}^{\text{II}}\text{Br}_2]_0/[\text{Me}_6\text{TREN}]_0/[\text{Na}_2\text{S}_2\text{O}_4]_0 = 0.1/0.1/1$  in a  $\text{MeOAc}/\text{EtOH} = 2/1$  (v/v) at  $30^\circ\text{C}$

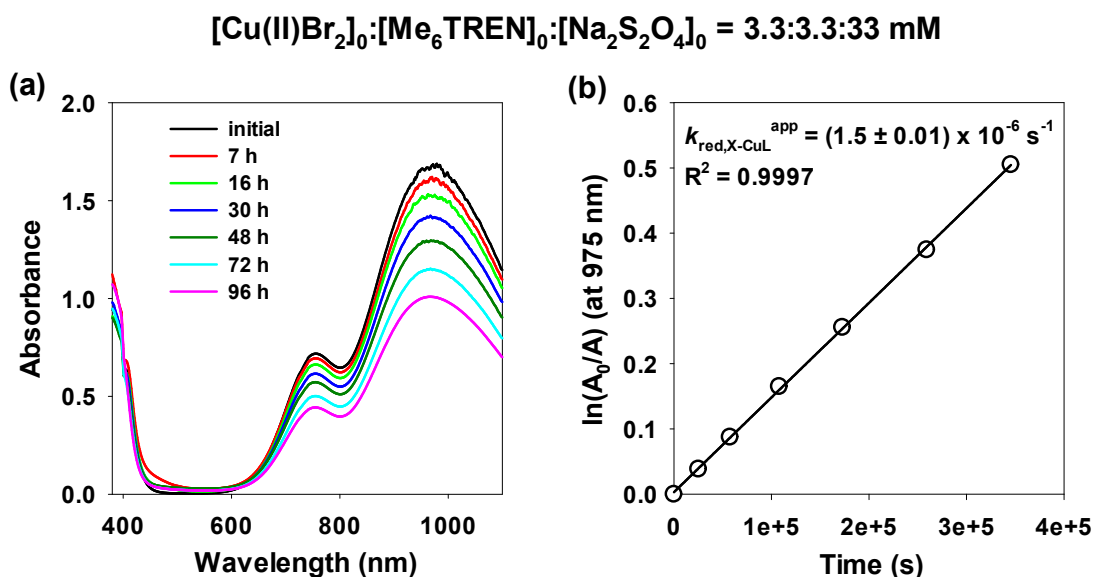


**Fig. S20.** (a) UV-Vis spectra of  $\text{Cu}^{\text{II}}\text{Br}_2/\text{Me}_6\text{TREN}$  during the reduction by  $\text{Na}_2\text{S}_2\text{O}_4$  in a  $\text{MeOAc}/\text{EtOH} = 2/1$  (v/v) mixture at  $30\text{ }^\circ\text{C}$  and (b) determination of the  $k_{\text{red},\text{X}-\text{CuL}}^{\text{app}}$ . Conditions:  $[\text{Cu}^{\text{II}}\text{Br}_2]_0/[\text{Me}_6\text{TREN}]_0/[\text{Na}_2\text{S}_2\text{O}_4]_0 = 0.1/0.1/1$ ;  $[\text{Cu}^{\text{II}}\text{Br}_2]_0 = 3.3\text{ mM}$

### Reduction rates of Alkyl Halides and Copper Complexes vs. their Redox Potentials

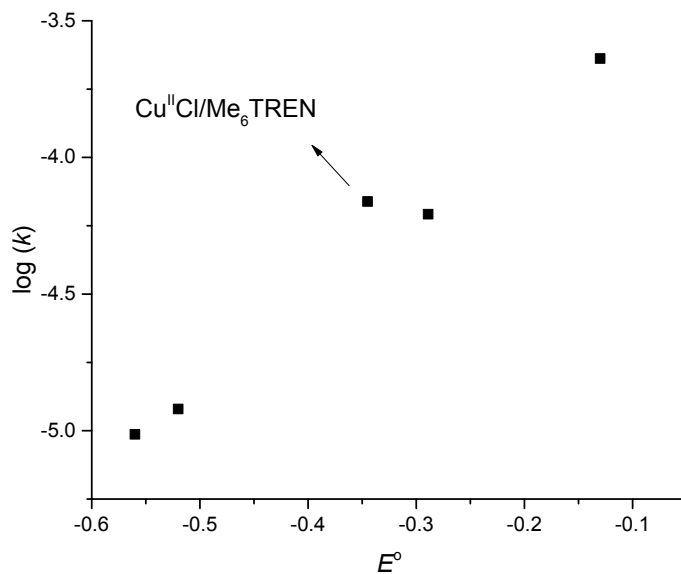


**Fig. S21.** Plot of logarithm of the apparent reduction rate of substrates in Table 3 vs. their redox potential.

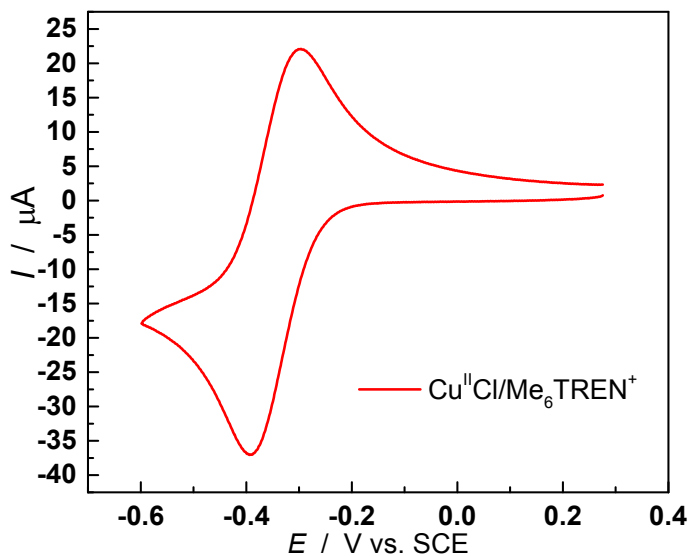


**Fig. S22.** CV of  $2 \times 10^{-3}$  M  $\text{Cu}^{\text{II}}\text{Cl}_2/\text{Me}_6\text{TREN}$  in  $\text{MA}/\text{EtOH}/\text{H}_2\text{O} = 2/0.9/0.1$  (v/v/v) + 0.1 M  $n\text{-Bu}_4\text{NPF}_6$ , recorded at  $30^\circ\text{C}$  and  $\nu = 0.1 \text{ V s}^{-1}$ .

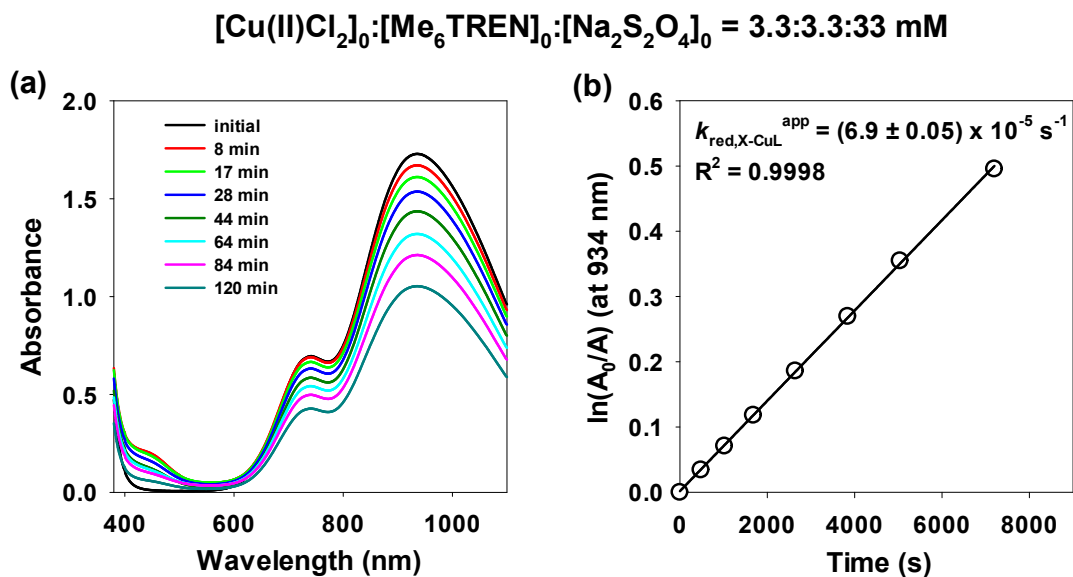


**Fig. S23.** (a) UV-Vis spectra of  $\text{Cu}^{\text{II}}\text{Cl}_2/\text{Me}_6\text{TREN}$  during the reduction by  $\text{Na}_2\text{S}_2\text{O}_4$  in a  $\text{MeOAc}/\text{EtOH}/\text{H}_2\text{O} = 2/0.9/0.1$  (v/v/v) mixture at  $30^\circ\text{C}$  and (b) determination of the  $k_{\text{red,X-CuL}}^{\text{app}}$ . Conditions:  $[\text{Cu}^{\text{II}}\text{Cl}_2]_0/[\text{Me}_6\text{TREN}]_0/[\text{Na}_2\text{S}_2\text{O}_4]_0 = 0.1/0.1/1$ ;  $[\text{Cu}^{\text{II}}\text{Cl}_2]_0 = 3.3 \text{ mM}$

## References

1. Bortolamei, N.; Isse, A. A.; Di Marco, V. B.; Gennaro, A.; Matyjaszewski, K. Thermodynamic Properties of Copper Complexes Used as Catalysts in Atom Transfer Radical Polymerization. *Macromolecules* **2010**, 43 (22), 9257-9267 DOI: 10.1021/ma101979p.
2. Konkolewicz, D.; Kryszewski, P.; Góis, J. R.; Mendonça, P. V.; Zhong, M.; Wang, Y.; Gennaro, A.; Isse, A. A.; Fantin, M.; Matyjaszewski, K. Aqueous RDRP in the Presence of Cu<sup>0</sup>: The Exceptional Activity of CuI Confirms the SARA ATRP Mechanism. *Macromolecules* **2014**, 47 (2), 560-570 DOI: 10.1021/ma4022983.
3. Matyjaszewski, K.; Paik, H.-j.; Zhou, P.; Diamanti, S. J. Determination of Activation and Deactivation Rate Constants of Model Compounds in Atom Transfer Radical Polymerization. *Macromolecules* **2001**, 34 (15), 5125-5131 DOI: 10.1021/ma010185+.
4. Bowry, V. W.; Ingold, K. U. Kinetics of nitroxide radical trapping. 2. Structural effects. *J. Am. Chem. Soc.* **1992**, 114 (13), 4992-4996 DOI: 10.1021/ja00039a006.
5. Skene, W. G.; Scaiano, J. C.; Listigovers, N. A.; Kazmaier, P. M.; Georges, M. K. Rate Constants for the Trapping of Various Carbon-Centered Radicals by Nitroxides: Unimolecular Initiators for Living Free Radical Polymerization. *Macromolecules* **2000**, 33 (14), 5065-5072 DOI: 10.1021/ma991753c.
6. Bard, A. J.; Faulkner, L. R., *Electrochemical methods: Fundamentals and applications*, 2nd Edition. Wiley: Hoboken, NJ, 2000.
7. Isse, A. A.; Berzi, G.; Falciola, L.; Rossi, M.; Mussini, P. R.; Gennaro, A. Electrocatalysis and electron transfer mechanisms in the reduction of organic halides at Ag. *J. Appl. Electrochem.* **2009**, 39 (11), 2217 DOI: 10.1007/s10800-008-9768-z.

8. Wang, Y.; Kwak, Y.; Buback, J.; Buback, M.; Matyjaszewski, K. Determination of ATRP Equilibrium Constants under Polymerization Conditions. *ACS Macro Letters* **2012**, 1 (12), 1367-1370 DOI: 10.1021/mz3005378.
9. Buback, M.; Kuelpmann, A.; Kurz, C. Termination Kinetics of Methyl Acrylate and Dodecyl Acrylate Free-Radical Homopolymerizations up to High Pressure. *Macromol. Chem. Phys.* **2002**, 203 (8), 1065-1070 DOI: 10.1002/1521-3935(20020501)203:8<1065::AID-MACP1065>3.0.CO;2-F.